

## Article

# Adsorption of Pesticides on Activated Carbons from Peach Stones

Souha Harabi <sup>1</sup>, Sami Guiza <sup>1</sup> , Ariadna Álvarez-Montero <sup>2</sup> , Almudena Gómez-Avilés <sup>2</sup> , Mohamed Bagané <sup>1</sup>, Carolina Belver <sup>2</sup>  and Jorge Bedia <sup>2,\*</sup> 

<sup>1</sup> Applied Thermodynamics Research Laboratory, National Engineering School of Gabes, University of Gabes, Gabes 6029, Tunisia; souhaharrabi20@gmail.com (S.H.); sami\_guiza@yahoo.fr (S.G.); drmbag1420@yahoo.fr (M.B.)

<sup>2</sup> Chemical Engineering Department, Universidad Autónoma de Madrid, Campus Cantoblanco, E-28049 Madrid, Spain; ariadna.alvarez@uam.es (A.Á.-M.); almudena.gomez@uam.es (A.G.-A.); carolina.belver@uam.es (C.B.)

\* Correspondence: jorge.bedia@uam.es

**Abstract:** This study analyzes the adsorption of two model pesticides, namely, 2,4-dichlorophenoxyacetic acid (2,4-D) and carbofuran on activated carbons obtained by chemical activation with phosphoric acid of peach stones. The effect of the synthesis conditions on the surface area development was analyzed. The highest surface area was obtained with an impregnation time of 5 h, an impregnation ratio equal to 3.5, an activation temperature of 400 °C, and 4.5 h of activation time. Under these conditions, the maximum specific surface area was equal to 1182 m<sup>2</sup>·g<sup>-1</sup> which confirms the high porosity of the activated carbon, predominantly in the form of micropores. The surface chemistry of this activated carbon was also characterized using pH at point of zero charge, scanning electron microscopy, and Fourier transform infrared spectroscopy. Both kinetics and equilibrium adsorption tests were performed. Adsorption kinetics confirmed that 2,4-D adsorption follows a pseudo first-order adsorption kinetic model, while carbofuran adsorption is better described by a pseudo second-order one. Regarding the equilibrium adsorption, a higher adsorption capacity is obtained for 2,4-D than carbofuran (c.a. 500 and 250 mg·g<sup>-1</sup>, respectively). The analysis of the thermodynamics and characterization after use suggest a predominantly physisorption nature of the process.



**Citation:** Harabi, S.; Guiza, S.; Álvarez-Montero, A.; Gómez-Avilés, A.; Bagané, M.; Belver, C.; Bedia, J. Adsorption of Pesticides on Activated Carbons from Peach Stones. *Processes* **2024**, *12*, 238. <https://doi.org/10.3390/pr12010238>

Academic Editors: Chang Min Kim and Made Sucipta

Received: 21 December 2023

Revised: 11 January 2024

Accepted: 21 January 2024

Published: 22 January 2024



**Copyright:** © 2024 by the authors. Licensee MDPI, Basel, Switzerland. This article is an open access article distributed under the terms and conditions of the Creative Commons Attribution (CC BY) license (<https://creativecommons.org/licenses/by/4.0/>).

**Keywords:** activated carbon; adsorption; pesticides; carbofuran; 2,4-dichlorophenoxyacetic acid; isotherms; kinetics

## 1. Introduction

Aquatic ecosystems are the principal receptors of contaminants [1], which are discharged directly or indirectly from diverse natural and human-caused sources, including both industrial and municipal wastewater [2,3]. Their contamination represents a threat to human health due to the potential health dangers produced by many different types of pollutants [4,5]. Among these pollutants, pesticides are worldwide used for the regulation of parasites in agricultural soils and for the control of insects that can cause and disseminate some serious diseases [3]. Due to their persistence, they can bioaccumulate in soils [6] and foods and can pose a threat to animal and human health [7]. Among various pesticides, we selected 2,4-dichlorophenoxyacetic acid (2,4-D) and carbofuran as model pesticide pollutants since they are widely used in the formulation of herbicides and insecticides, respectively. The 2,4-D is an anionic pesticide, highly selective [8], and poorly biodegradable [9,10]. It is a herbicide that kills dicots without affecting monocots and mimics natural auxin at the molecular level. It is widely used, and consequently, it is commonly detected in water lots, and in different soils. The World Health Organization (WHO) establishes the upper allowable concentration for 2,4-D in potable water at 20 µg·L<sup>-1</sup> [11]. On the other hand, carbofuran (2,3-dihydro-2,2-dimethyl-7-benzofuranyl), is a highly toxic N-methyl carbamate insecticide [12,13]. It is being widely applied in the agronomic field for its proven

efficiency in controlling insects [7]. Carbofuran is an insecticide that poisons arthropods by inhibiting the action of a specific acetylcholine esterase enzyme. In addition, this pesticide is quite persistent in the ground and aqueous ecosystems under neutral or acidic conditions. Therefore, it is considered exceedingly harmful to both birds and aquatic animals [14].

In this context, it is vital to look for effective methods to remove these hazardous products from water [9]. We mention, for example, membrane separation, flocculation, ozonation, coagulation, aerobic and anaerobic treatment [15], chemical precipitation, solvent extraction, ion-exchange capacity, photocatalytic activity [16] and adsorption [17,18]. Compared with the different available technologies for the removal of pesticides, adsorption is the most analyzed due to its flexibility, simplicity, low cost, and easiness of use [9,19,20]. In addition, it is known for its low consumption of energy and relatively high adsorption capacity [21]. Among the different adsorbents [22–24], activated carbons have some clear advantages [25–27], namely, they can be synthesized from renewable materials (biomass), are of relatively low cost [19,28], and usually show well-developed and tunable porosity [16]. Activated carbon can be obtained through two different activation methods: physical and chemical activation [29]. Physical activations consist of the partial gasification of the carbonaceous precursor using water vapor, carbon dioxide or oxygen. The removal of the carbon atoms during the gasification reaction results in the formation of porosity. Chemical activation is produced through the impregnation of the carbonaceous precursor with an activating agent. During the subsequent heating, the precursor suffers from dehydration and oxidation reactions; therefore, carbonization and activation take place simultaneously. Different chemical activating agents have been used, such as  $H_3PO_4$ ,  $ZnCl_2$ ,  $FeCl_3$  or  $KOH$ . Chemical activation usually results in higher yields. Phosphoric acid activation results in activated carbon with an acidic surface that can be very suitable for some specific applications [30–32].

The main objective of this study is to synthesize activated carbons from peach stones through chemical activation with phosphoric acid. The effect of different synthesis parameters, namely, impregnation time, impregnation ratio (mass ratio of activating agent to carbon precursor), activation temperature and activation time, on the surface area of the resulting carbon was analyzed. The activated carbon with the highest surface area was further used for the adsorption of 2,4-D and carbofuran. Different kinetic and thermodynamic models were used to fit the experimental adsorption data.

## 2. Materials and Methods

### 2.1. Materials

All chemical products needed were obtained from Sigma Aldrich and employed without any added purification. The phosphoric acid ( $H_3PO_4$ ) with 85% of purity was used for activated carbon synthesis. Equally, both pesticides, carbofuran ( $C_{12}H_{15}NO_3$ ) and 2,4-dichlorophenoxyacetic acid ( $C_8H_6Cl_2O_3$ ) were obtained from this company and used for the adsorption studies.

### 2.2. Preparation of Activated Carbons

Peach stones were collected and washed several times with water to eliminate the impurities. Then, the stones were crushed and sieved (particle size between 100 and 125  $\mu m$ ), and dried for 24 h at 105 °C. The material was subjected to a chemical activation method with phosphoric acid (50%) in a tubular horizontal furnace. The dried stones were physically mixed with a variable amount of phosphoric acid (impregnation ratios between 3 and 5) at different impregnation times (4–6 h). Next, the heterogeneous mixture was introduced in a tubular furnace and heated at 10 °C·min<sup>-1</sup> up to the activation temperature (300–600 °C) and maintained at this temperature during the activation time (3–5 h). After cooling down, the samples were washed with distilled water to remove the remains of the activating agent and reaction byproduct and to free the newly developed porous texture. The experimental design provides the possibility of optimizing the parameters and minimizing the error with a reduced number of experiences [33,34]. In the current study,

experiments with the specific surface area as a response were designed with the Central Composite Design (CCD) with four, two-level, factors using Design-Expert 13 software with 30 essays.

### 2.3. Characterization Techniques

Elemental analyses were conducted in a LECO CHNS-932 apparatus to quantify the content of C, N, and H in the activated carbon. N<sub>2</sub> adsorption isotherms were acquired at −196 °C with a Micromeritics TriStar II instrument to quantitatively examine the pore structure of the optimized activated carbon. The solid samples (weight between 100 and 150 mg) were degasified at 150 °C during 24 h. The specific surface area was lastly determined by the Brunauer–Emmett–Teller (BET) method. The micropore volume and external surface area were obtained using the t-method applied to the adsorption branch of the isotherm. Finally, the total pore volume was estimated from the amount of N<sub>2</sub> adsorbed at relative pressures close to 1 transformed in liquid volume.

Fourier Transform Infrared Spectroscopy (FTIR) analyses were carried out with a Bruker Vertex 70 V spectrophotometer by transmission using KBr pellets in the wavenumber range from 400 to 4000 cm<sup>−1</sup>.

The pH at the point of zero charge (pH<sub>PZC</sub>) was quantified using the pH drift method. Briefly, the pH value of several solutions of NaCl was adjusted from 1 to 13 using HCl (0.1 M) or NaOH (0.1 M). The activated carbon (20 mg) was suspended in the different solutions and bubbled with N<sub>2</sub> for 5 min to eliminate the gases dissolved in the solutions. After 48 h under stirring, the pH was measured and represented versus the initial one, corresponding to the intersection of the line with the diagonal to the pH<sub>PZC</sub> value.

Scanning Electron Microscopy (SEM) was performed to identify the morphology of the selected activation carbon. The sample was covered with a 4 nm layer of platinum in Leica EM ACE600 equipment and was measured in a FESEM TESCAN CLARA microscopy with ultra-high resolution at 15 KV and an ET detector.

Thermogravimetric Analyses (TGA/TDA) were investigated for the thermal stability of the best activated carbon in an SDT650 TA instrument, using a 10 °C·min<sup>−1</sup> heating rate up to 900 °C under a 100 mL·min<sup>−1</sup> continuous air atmosphere.

### 2.4. Adsorption Tests

The selected activated carbon (that with the highest BET surface area) was used to test the adsorption from aqueous solution of two model pesticides, 2,4-D and carbofuran. Batch equilibrium tests were conducted at different temperatures (25, 45, and 65 °C) with a volume equal to 250 mL of aqueous solution at various initial concentrations of the pesticide ranging from 5 to 100 mg·L<sup>−1</sup> with 50 mg·L<sup>−1</sup> of the activated carbon. After 24 h of controlled temperature and agitation (200 rpm), the solutions were filtered and finally, the remaining concentration of the corresponding pesticide in the liquid solution phase was analyzed by UV-Vis. Also, adsorption kinetic experiments were performed in the same batch system with an initial pesticide concentration of 20 mg·L<sup>−1</sup> with the same solution volume, activated carbon concentration, and temperatures mentioned previously for the equilibrium trials.

## 3. Results and Discussion

### 3.1. Characterization of Activated Carbons

The optimization of the activated carbon preparation procedure from peach stones was carried out. The selection of the best activated carbon was made based on the maximization of the specific surface area, as a response, to the experiences of the CCD plan. Table 1 shows some results for the textural properties of activated carbons prepared at different conditions. As can be seen, in all cases, the specific surface area was high, achieving the sample AC5\_4.5\_400\_4.5, that synthesized with an impregnation time of 5 h, at an impregnation ratio of 4.5, an activation temperature of 400 °C and activation time of 4.5 h, the highest total surface area (1182 m<sup>2</sup>·g<sup>−1</sup>). This value was higher than the values found in the literature for acti-

vated carbons prepared from the same precursor. For example, Pérez-Rodríguez et al. [35] obtained a specific surface area value of  $846 \text{ m}^2 \cdot \text{g}^{-1}$  for activated carbon obtained from peach stones through physical activation with water vapor, and the values presented by Kozyatnyk et al. [36] did not exceed  $500 \text{ m}^2 \cdot \text{g}^{-1}$  when activating peach stones with  $\text{CO}_2$ . Since AC5\_4.5\_400\_4.5 showed the highest surface area and the most developed porous texture, it was selected for the following adsorption tests and a complete characterization.

**Table 1.** Porous texture parameters.

| Sample          | Impregn. Time (h) | Impregn. Ratio | Activation Temperature ( $^{\circ}\text{C}$ ) | Activation Time (h) | BET ( $\text{m}^2 \cdot \text{g}^{-1}$ ) | Sext ( $\text{m}^2 \cdot \text{g}^{-1}$ ) | Vmicro ( $\text{cm}^3 \cdot \text{g}^{-1}$ ) | Vtotal ( $\text{cm}^3 \cdot \text{g}^{-1}$ ) |
|-----------------|-------------------|----------------|---|---------------------|--|---|--|--|
| AC5_3.5_400_4.5 | 5                 | 3.5            | 400   | 4.5                 | 782                                      | 215                                       | 0.271  | 0.398  |
| AC5_4.5_400_3.5 | 5                 | 4.5            | 400   | 3.5                 | 631                                      | 232                                       | 0.188  | 0.327  |
| AC5_4.5_400_4.5 | 5                 | 4.5            | 400   | 4.5                 | 1182                                     | 413                                       | 0.367  | 0.609  |
| AC6_4.5_400_4.5 | 6                 | 4.5            | 400   | 4.5                 | 584                                      | 187                                       | 0.188  | 0.290  |

Figure 1 depicts the  $\text{N}_2$  adsorption–desorption isotherm of the ACs with highest surface areas. The isotherm showed the typical shape of type I according to the IUPAC classification [37]. This type of isotherm corresponds to a predominantly microporous solid with some minor contribution of mesoporosity. This is confirmed by the low value of external ( $S_{\text{ext}}$ ) compared to the BET surface areas as well as the higher proportion of micropore ( $V_{\text{micro}}$ ) in the total pore volume ( $V_{\text{pore}}$ ) [37–39], as can be seen in Table 1.

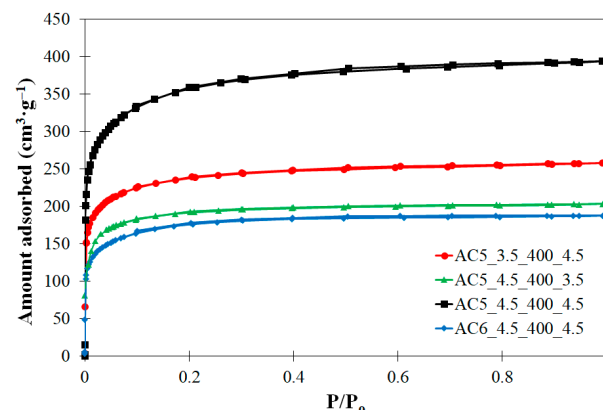


**Figure 1.**  $\text{N}_2$  adsorption–desorption isotherm at 77 K.

The results of the elemental analysis of peach stone precursor and AC5\_4.5\_400\_4.5 are collected in Table 2. After activation of raw material, the carbon content increases and becomes close to 80%, while the percentages of hydrogen, oxygen, and nitrogen decrease. This can be justified by the removal of the molecules of water and the decomposition/devolatilization of the precursor during the activation stage. The ash content increased slightly with activation, although it remains very low (lower than 5%). These results agree with others found in the literature for activated carbons obtained from the same raw material [40–44].

**Table 2.** Elemental analysis of peach precursor and AC5\_4.5\_400\_4.5 activated carbon.

| Sample          | % C   | % H  | % N  | % O <sup>1</sup> | % Ash |
|-----------------|-------|------|------|------------------|-------|
| Peach           | 44.42 | 5.62 | 0.91 | 46.23            | 2.86  |
| AC5_4.5_400_4.5 | 77.95 | 3.06 | 0.31 | 13.95            | 4.73  |

<sup>1</sup> Obtained by difference.

Thermogravimetric analyses for both activated carbon and raw material were conducted in the temperature range from 30 to 900 °C under an air atmosphere (Figure 2). Three major steps were observed in the case of the raw peach stone. The first one, from 30 to 100 °C corresponds to the lowest reduction in weight (less than 7%), and is associated with the removal of water molecules (dehydration). The highest value of weight reduction was found during the second step for temperatures ranging from 100 to 500 °C and it can be explained by the oxidation of cellulose and hemicellulose in the peach stone. Finally, the last part of the curve is expected to correspond to the oxidation of lignin, the most stable biopolymer in biomass. In the case of the activated carbon, the TG profile is clearly displaced to very significantly higher temperatures due to the previous devolatilization of part of the organic matter during the activation step at 400 °C. Only a negligible mass loss (most likely associated with the loss of humidity) is obtained below the activation temperature. Above 500 °C, a dramatic mass loss is observed due to the fast combustion of the organic matter in the carbon structure. It is worth mentioning the high oxidation resistance of this activated carbon with no significant mass loss up to temperatures close to 500 °C. This is a consequence of the formation of different phosphate groups on the activated carbon surface that are responsible for this enhancement of the oxidation resistance as confirmed by previous studies [45,46].

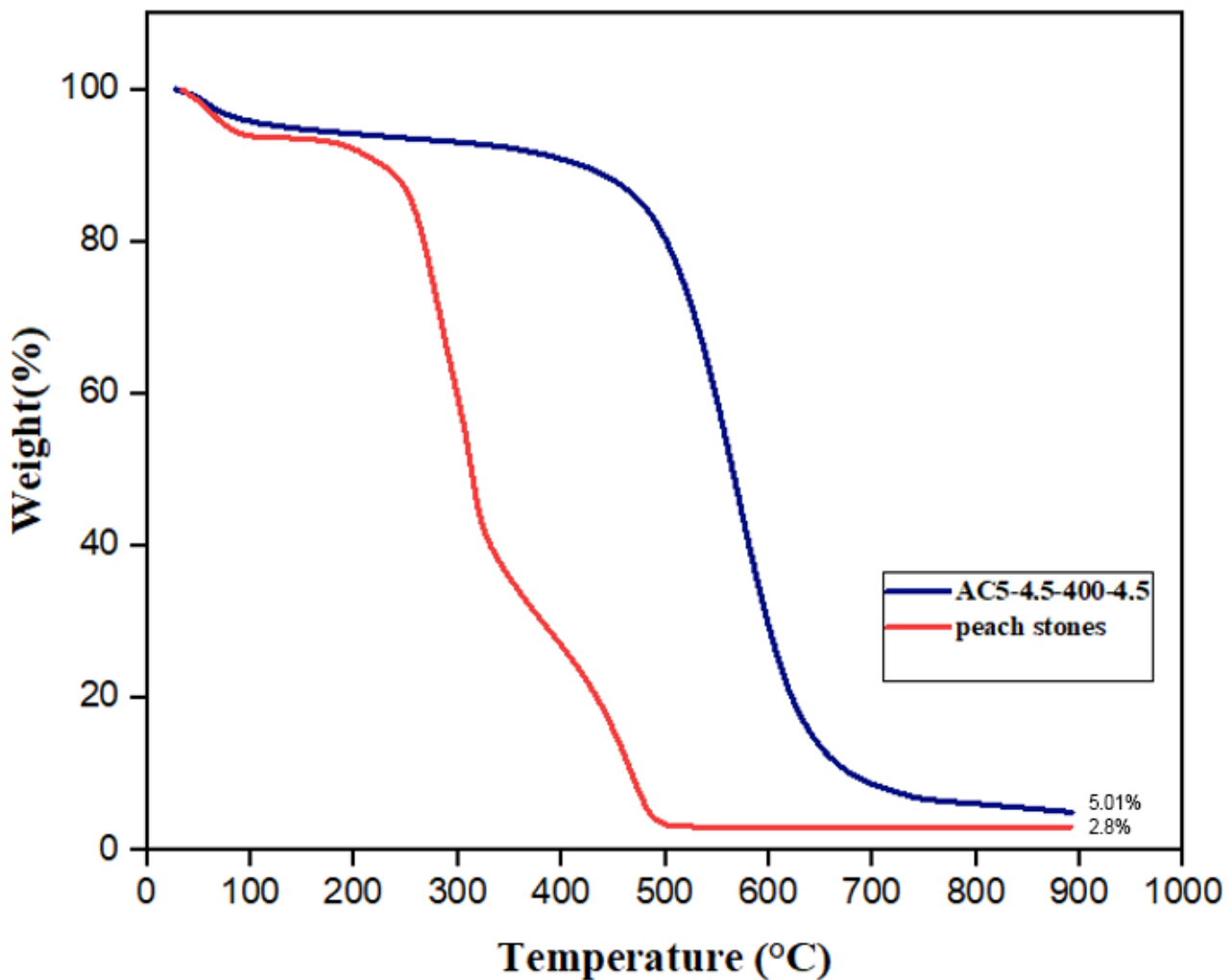


**Figure 2.** Thermogravimetric analysis of peach stones and AC5\_4.5\_400\_4.5.

Figure 3 shows the morphology of the activated carbon at different resolutions. SEM images highlighted the presence of many cavities that would allow for faster access to the

internal porosity of the activated carbon improving the kinetics of the adsorption process. This morphology is characteristic of activated carbons obtained from biomass precursors, with high cavities coming from the original structure of the biomass precursor [47,48].

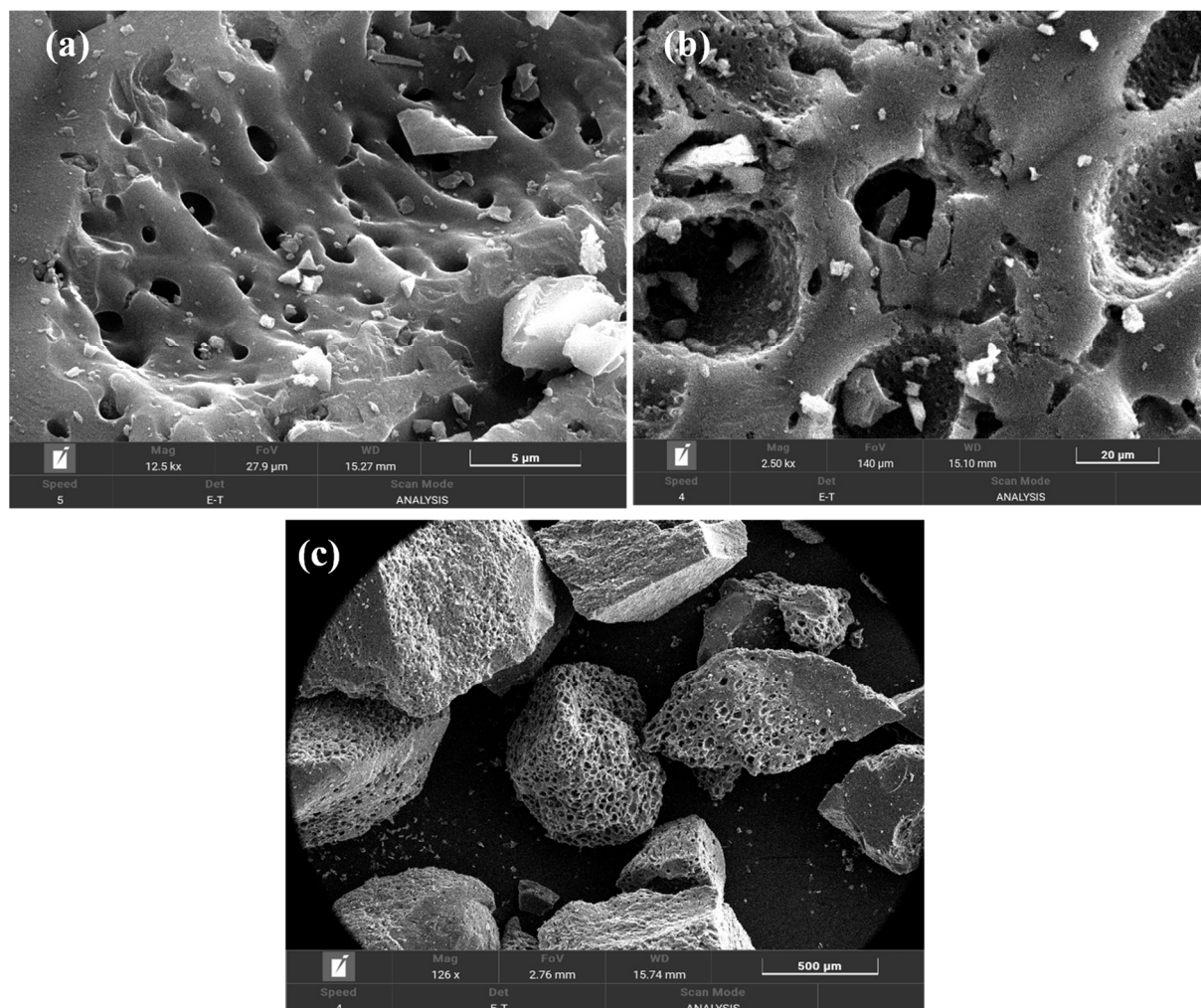


**Figure 3.** SEM images of AC5\_4.5\_400\_4.5 (a) = 5  $\mu\text{m}$ ; (b) = 20  $\mu\text{m}$ ; (c) = 500  $\mu\text{m}$ .

Besides the morphological and textural properties, the surface charge and functional groups are significant for the understanding of the adsorption mechanism. Figure 4 represents the evolution of the final pH of the solution versus the initial value for the activated carbon. The  $\text{pH}_{\text{PZC}}$  of the activated carbon was 4.3 characteristic of an acidic surface. It is expected that the activation with phosphoric acid resulted in an acidic carbon surface. Therefore, in aqueous solutions at a pH higher than 4.3, the activated carbon surface would be charged negatively, while it would be charged positively for a pH lower than this value. The  $\text{pK}_a$  value of 2,4-D was approximately equal to 2.8, resulting in the speciation diagram represented in Figure 5a. Consequently, at pH values lower than 2.8, the 2,4-D pesticide molecules are in a molecular state, and therefore no electrostatic interactions between the positively charged surface of the carbon and 2,4-D molecules are expected [49]. In contrast, at pH values higher than 4.3, a certain electrostatic repulsion would be expected for the 2,4-D adsorption. In the case of carbofuran, the  $\text{pK}_a$  of this pesticide is 11.9 [50]; therefore, carbofuran is a non-ionic pesticide, without strong acidic or basic functionalities and it does not dissociate in the solution (except at a very basic pH higher than 11.9, see speciation diagram in Figure 5b) indicating that no electrostatic interactions would exist between carbofuran and the activated carbon surface.

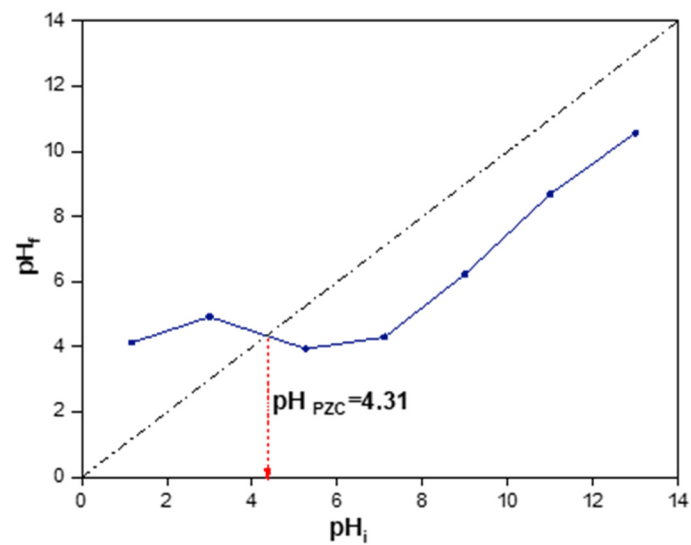


Figure 4.  $\text{pH}_{\text{PZC}}$  of AC5\_4.5\_400\_4.5.

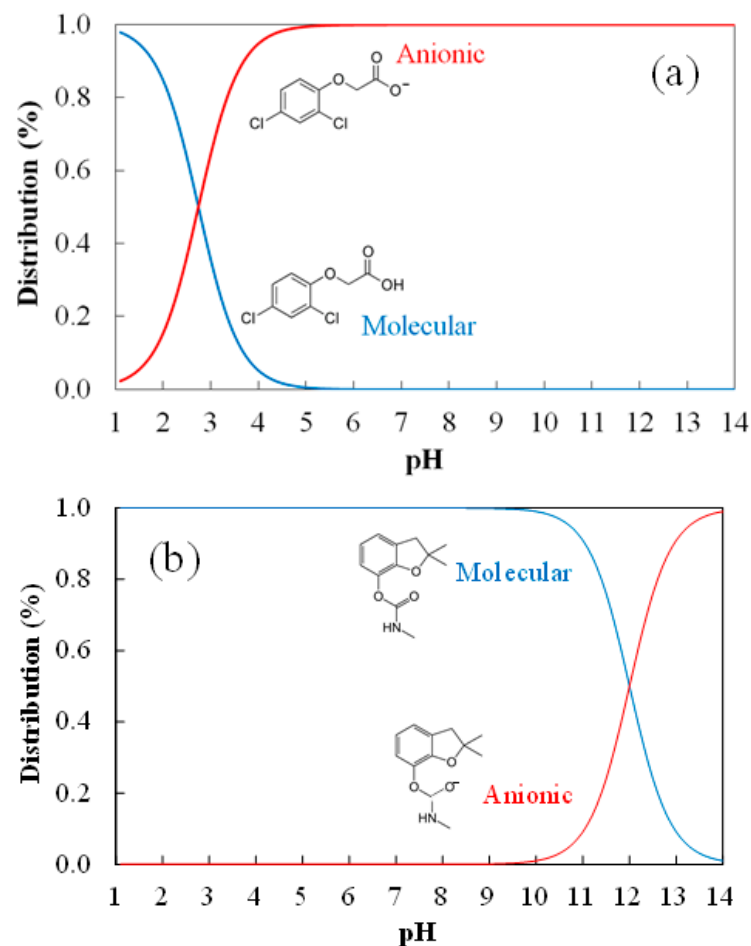
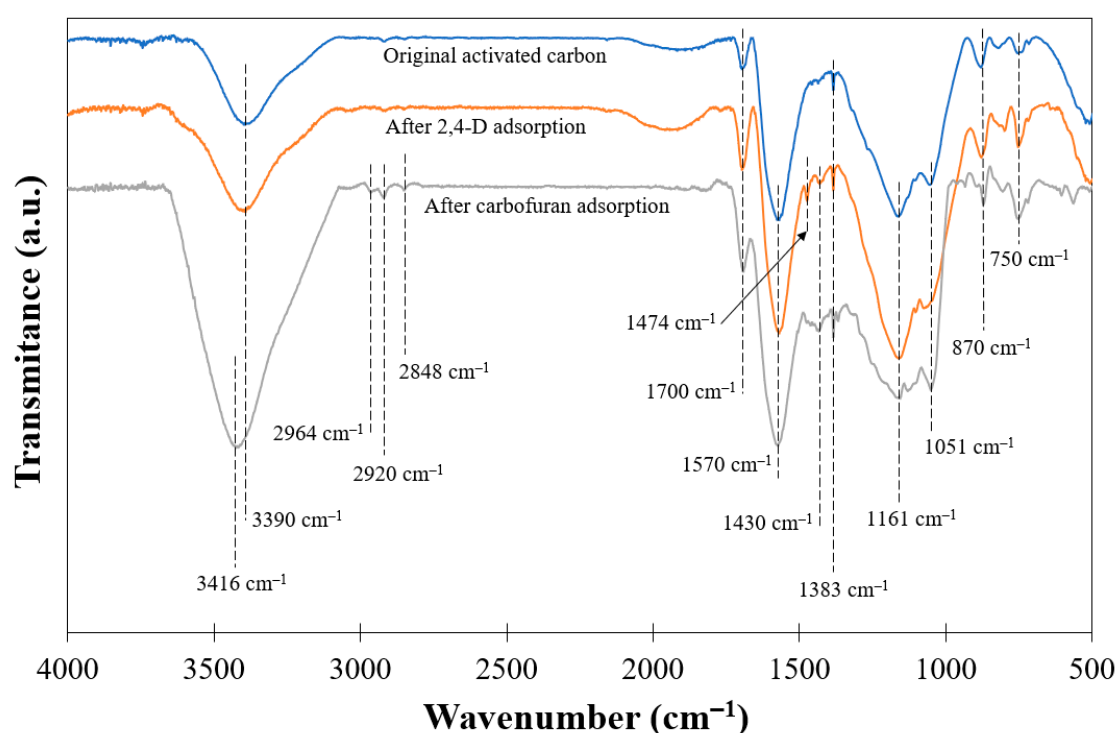


Figure 5. Speciation diagram of (a) 2,4-dichlorophenoxyacetic acid and (b) carbofuran.

Figure 6 represents the FTIR spectra of the original activated carbon and after its use in 2,4-D and carbofuran adsorption. The spectrum of the original carbon shows a limited number of bands. This is expected since the increase in the temperature during the activation step removes part of the functional groups in the form of volatile matter. The strong band centered at around  $3390\text{ cm}^{-1}$  is associated with the stretching vibrations

of the O–H bonds, usually due to the presence of surface hydroxyl groups or adsorbed water molecules. The asymmetry of this band at lower wavenumbers is characteristic of the presence of strong hydrogen bonds. The broad band at  $1570\text{ cm}^{-1}$  corresponds to C–C vibrations in aromatic rings. The last broad band at  $1161\text{ cm}^{-1}$  can be ascribed to C–O stretching in acids, alcohols, phenols, ethers, and/or esters groups [51]. However, it is also characteristic of phosphorous, and phosphor carbonaceous compounds present in the phosphoric acid-activated carbons, such as the stretching vibration of hydrogen-bonded P=O, to O–C stretching vibrations in P–O–C (aromatic) linkage, and to P=OOH [52]. The band at around  $1700\text{ cm}^{-1}$  is related to the C=O stretching vibrations of carboxyl or carbonyl groups, while those at  $1430$  and  $1380\text{ cm}^{-1}$  are characteristic of the C=C vibrations of the aromatic rings [53]. The band centered at  $1050\text{ cm}^{-1}$  may be ascribed to the asymmetrical stretch vibrations of C–O–C groups [54]. In the low wavenumber region, the bands at  $870$  and  $750\text{ cm}^{-1}$  can be related to the out-of-plane bending of C–H groups in the aromatic rings [55].



**Figure 6.** FTIR diagrams for AC5\_4.5\_400\_4.5 before and after adsorption.

### 3.2. Adsorption Isotherms

Figures 7 and 8 represent the adsorption isotherms at three different temperatures ( $25$ ,  $45$ , and  $65\text{ }^{\circ}\text{C}$ ) of 2,4-D and carbofuran, respectively. The tests were performed at natural pH (c.a. 6.0). The isotherms correspond to type L according to Giles classification [56] characteristics of a strong interaction between the molecules of adsorbate and adsorbent and weak interaction between the molecules of adsorbates [57]. In this type of adsorption isotherm, the initial curvature shows that as more sites in the substrate are filled, it becomes increasingly difficult for the adsorbate molecules to find vacant sites. It can also be observed that the increase in the adsorption temperature results in an increase in the amounts adsorbed for both pesticides, suggesting an endothermic character of the adsorption process. If we compare the adsorption capacities of the two pesticides, it is concluded that those of 2,4-D are significantly higher than the corresponding ones of carbofuran in agreement with previous studies [5,58]. This can be explained on the basis of donor–acceptor mechanism between the negatively charged oxygen of the carbonyl groups of 2,4-D molecule (which is

in anionic state at the natural pH used in the tests, while carbofuran is in molecular form, see Figure 5) and some surface oxygenated groups of the activated carbon surface.

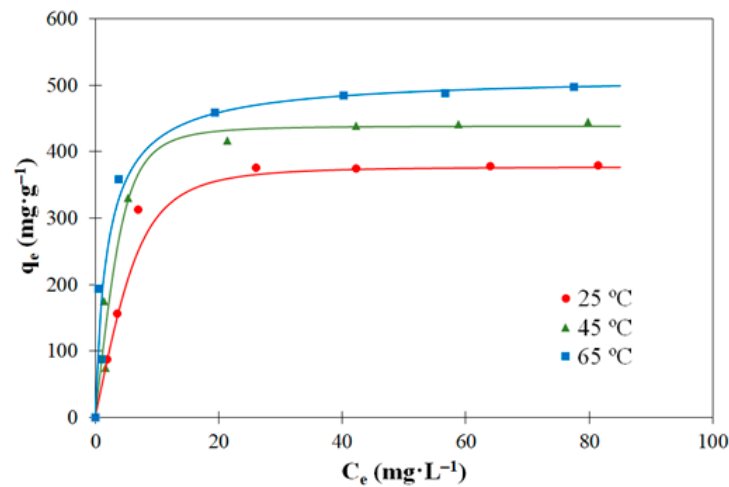


**Figure 7.** Experimental data (symbols) and Toth model's fitting (solid lines) for the adsorption equilibrium of 2,4-D on the activated carbon ( $C_0 = 250 \text{ mg}\cdot\text{L}^{-1}$ ;  $V = 250 \text{ mL}$ ).

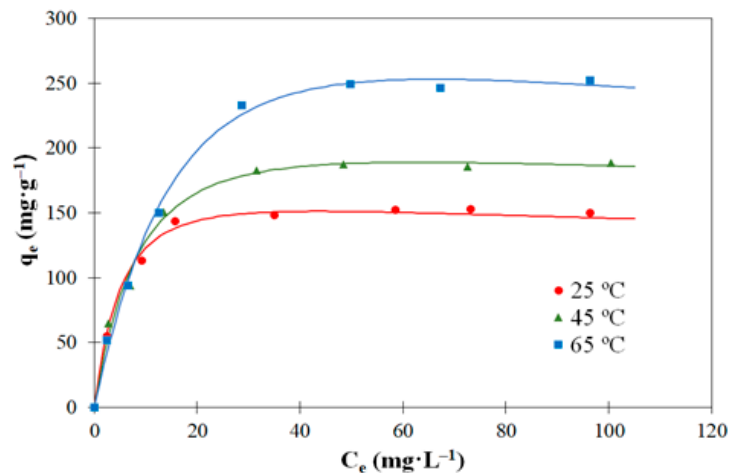


**Figure 8.** Experimental data (symbols) and Redlich–Peterson model's fitting (solid lines) for the adsorption equilibrium of carbofuran on the activated carbon ( $V = 250 \text{ mL}$ ;  $C_0 = 250 \text{ mg}\cdot\text{L}^{-1}$ ).

The adsorption capacities of both pesticides have been compared with those obtained in previous studies with different adsorbents. Hameed et al. [10] reported a 2,4-D adsorption capacity of  $238.1 \text{ mg}\cdot\text{g}^{-1}$  at  $30 \text{ }^\circ\text{C}$  on an activated carbon from KOH chemical activation of date stones. Lazarotto et al. [59] achieved an adsorption capacity of  $250.8 \text{ mg}\cdot\text{g}^{-1}$  at  $35 \text{ }^\circ\text{C}$  and pH 4 on mushroom-derived activated carbon synthesized by chemical activation with zinc chloride. Other different studies can be found in the literature, most of them reporting 2,4-D adsorption capacities significantly lower than those obtained in the current study (between  $350$  and  $500 \text{ mg}\cdot\text{g}^{-1}$ , depending on the adsorption temperature). In the case of carbofuran, Njoku et al. [48] found a maximum adsorption capacity of  $198.4 \text{ mg}\cdot\text{g}^{-1}$  when using activated carbon from coconuts activated with phosphoric acid. This value is similar to the adsorption capacity of carbofuran achieved in this work. However, other authors reported significantly lower adsorption capacities for the same compound. For example, J.M. Salman et al. reported values of  $96.1 \text{ mg}\cdot\text{g}^{-1}$  [5] and  $137.0 \text{ mg}\cdot\text{g}^{-1}$  [60] using a commercial granular activated carbon and a date seed activated carbon, respectively. The most plausible explanation for the higher adsorption capacities obtained by our activated

carbon is related to its high total surface area (close to 1200 m<sup>2</sup>·g<sup>-1</sup>), higher than those of the adsorbents used in the studies.

For the aim of investigating the relationship between equilibrium adsorbate and adsorbent concentrations, the experimental data were fitted with five empirical models (with two or three parameters), namely, Langmuir, Freundlich, Sips, Toth, and Redlich–Peterson. Table 3 shows their non-linear equations with the coefficients of correlation and the corresponding fitting parameters for both pesticides.

**Table 3.** Adsorption isotherms modeling for the 2,4-D and carbofuran pesticides.

| Models           | Non-Linear Expression                                      | Parameters  |   | R <sup>2</sup> |       |
|------------------|--|---|---|----------------|-------|
|                  |  | 2,4-D   | Carbofuran  |                |       |
| Langmuir         | $q_e = \frac{q_L * K_L * C_e}{1 + K_L * C_e}$              | T = 25 °C; q <sub>L</sub> = 417.4 mg/g;<br>K <sub>L</sub> = 0.22                  | T = 25 °C; q <sub>L</sub> = 163 mg/g;<br>K <sub>L</sub> = 0.25                    | 0.959          | 0.985 |
|                  |  | T = 45 °C; q <sub>L</sub> = 474.7 mg/g;<br>K <sub>L</sub> = 0.29                  | T = 45 °C; q <sub>L</sub> = 207.9 mg/g;<br>K <sub>L</sub> = 0.16                  | 0.958          | 0.987 |
|                  |  | T = 65 °C; q <sub>L</sub> = 508.8 mg/g;<br>K <sub>L</sub> = 0.49                  | T = 65 °C; q <sub>L</sub> = 296.7 mg/g;<br>K <sub>L</sub> = 0.086                 | 0.939          | 0.987 |
| Freundlich       | $q_e = K_F * C_e^n$  | T = 25 °C; K <sub>F</sub> = 140.9 mg/g;<br>n = 0.25                               | T = 25 °C; K <sub>F</sub> = 70.2 mg/g;<br>n = 0.19                                | 0.875          | 0.909 |
|                  |  | T = 45 °C; K <sub>F</sub> = 165.5 mg/g;<br>n = 0.25                               | T = 45 °C; K <sub>F</sub> = 68.2 mg/g;<br>n = 0.24                                | 0.887          | 0.927 |
|                  |  | T = 65 °C; K <sub>F</sub> = 208.9 mg/g;<br>n = 0.22                               | T = 65 °C; K <sub>F</sub> = 60.5 mg/g;<br>n = 0.34                                | 0.889          | 0.930 |
| Sips             | $q = \frac{q_s * (K_s * C_e)^n}{1 + (K_s * C_e)^n}$        | T = 25 °C; q <sub>s</sub> = 117.1 mg/g;<br>K <sub>s</sub> = 2.04 mg/g; n = 0.25   | T = 25 °C; q <sub>s</sub> = 62.0 mg/g;<br>K <sub>s</sub> = 1.78 mg/g; n = 0.19    | 0.995          | 0.996 |
|                  |  | T = 45 °C; q <sub>s</sub> = 140.9 mg/g;<br>K <sub>s</sub> = 1.86 mg/g; n = 0.24   | T = 45 °C; q <sub>s</sub> = 61.1mg/g;<br>K <sub>s</sub> = 1.47 mg/g; n = 0.24     | 0.969          | 0.991 |
|                  |  | T = 65 °C; q <sub>s</sub> = 178.3 mg/g;<br>K <sub>s</sub> = 2.02 mg/g; n = 0.22   | T = 65 °C; q <sub>s</sub> = 55.1 mg/g;<br>K <sub>s</sub> = 1.25 mg/g; n = 0.34    | 0.940          | 0.992 |
| Toth             | $\frac{q_e}{[1 + (K_T * C_e)^n]^{\frac{1}{n}}}$            | T = 25 °C; q <sub>T</sub> = 377.1 mg/g;<br>K <sub>T</sub> = 0.118 mg/g; n = 2.39  | T = 25 °C; q <sub>T</sub> = 153.8 mg/g;<br>K <sub>T</sub> = 0.16 mg/g; n = 1.67   | 0.998          | 0.997 |
|                  |  | T = 45 °C; q <sub>T</sub> = 438.4 mg/g;<br>K <sub>T</sub> = 0.185 mg/g; n = 2.40  | T = 45 °C; q <sub>T</sub> = 193.1 mg/g;<br>K <sub>T</sub> = 0.107 mg/g; n = 1.61  | 0.970          | 0.993 |
|                  |  | T = 65 °C; q <sub>T</sub> = 515.2 mg/g;<br>K <sub>T</sub> = 0.54 mg/g; n = 0.92   | T = 65 °C; q <sub>T</sub> = 256.2 mg/g;<br>K <sub>T</sub> = 0.06 mg/g; n = 2.20   | 0.939          | 0.996 |
| Redlich–Peterson | $q_e = \frac{q_{RP} * K_{RP} * C_e}{1 + (K_{RP} * C_e)^n}$ | T = 25 °C; q <sub>RP</sub> = 627.0 mg/g;<br>K <sub>RP</sub> = 0.10 mg/g; n = 1.22 | T = 25 °C; q <sub>RP</sub> = 225.4 mg/g;<br>K <sub>RP</sub> = 0.12 mg/g; n = 1.15 | 0.979          | 0.997 |
|                  |  | T = 45 °C; q <sub>RP</sub> = 612.6 mg/g;<br>K <sub>RP</sub> = 0.18 mg/g; n = 1.10 | T = 45 °C; q <sub>RP</sub> = 276.5 mg/g;<br>K <sub>RP</sub> = 0.09 mg/g; n = 1.15 | 0.965          | 0.994 |
|                  |  | T = 65 °C; q <sub>RP</sub> = 523.7 mg/g;<br>K <sub>RP</sub> = 0.46 mg/g; n = 1.01 | T = 65 °C; q <sub>RP</sub> = 425.9 mg/g;<br>K <sub>RP</sub> = 0.04 mg/g; n = 1.27 | 0.939          | 0.997 |

In the case of 2,4-D, Langmuir and Freundlich models presented high deviations with respect to the experimental data (specially Freundlich), which suggests that the ideal hypothesis of preferential monolayer coverage and energetic homogeneity of adsorption sites must be discarded. Toth model is the most adequate for the description of the experimental data as justified by the highest value of the correlation coefficient, although any of the three parameter models fit properly the experimental adsorption data. Toth model is typical of the adsorption of gas or organic compounds [61] and indicates that the adsorbent surface is heterogenous [62]. In the case of carbofuran adsorption, deviations were lower than those of 2,4-D, being Toth and Redlich–Peterson models the most suitable

for the description of the experimental adsorption equilibrium by the activated carbon. As it is mentioned in the literature [61,62], the Redlich–Peterson model can be used to describe both heterogeneous and homogeneous systems. Figures 7 and 8 represent the fitting of the 2,4-D and carbofuran adsorption experimental data (points) to Toth and Redlich–Peterson models (solid lines), respectively. As can be seen, these models fit the experimental results properly.

### 3.3. Adsorption Kinetics

Figures 9 and 10 represent the adsorption kinetic curves of 2,4-D and carbofuran at different temperatures (25, 45, and 65 °C), respectively. Adsorption was slow for both pesticides, requiring around 200 min to achieve equilibrium.

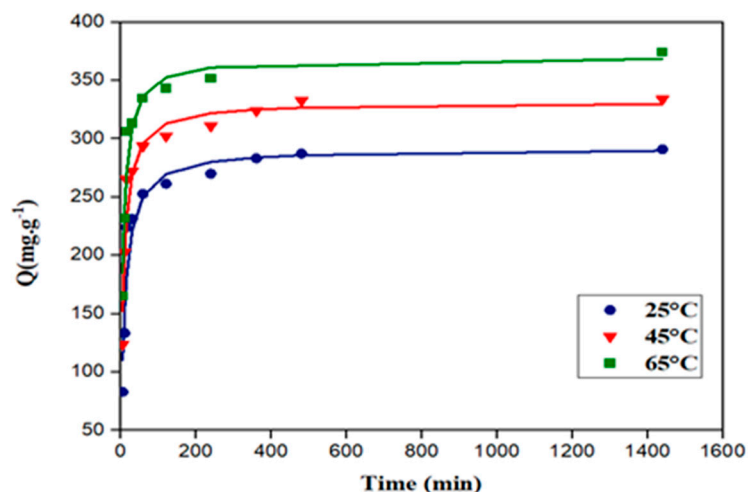


**Figure 9.** Kinetic curves of adsorption of 2,4-D on the activated carbon at 25, 45, and 65 °C. Symbols: experimental data; solid lines: fitting to pseudo first-order model ( $C_0 = 20 \text{ mg}\cdot\text{L}^{-1}$ ;  $V = 250 \text{ mL}$ ).

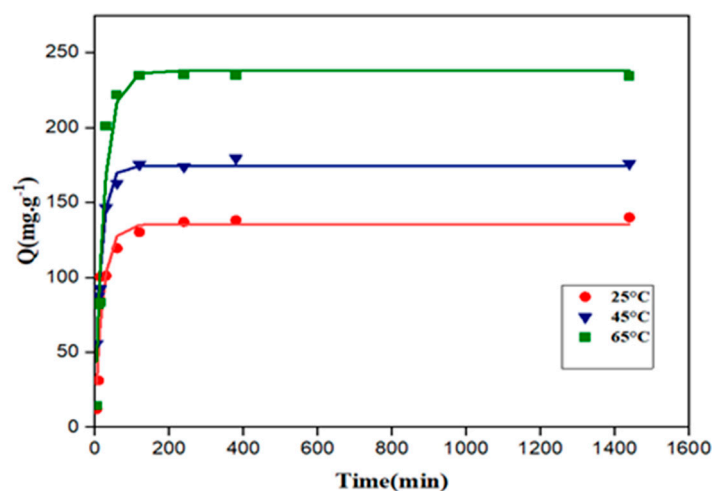


**Figure 10.** Kinetic curves of adsorption of 2,4-D on the activated carbon at 25, 45, and 65 °C. Symbols: experimental data; solid lines: fitting to second-order model ( $C_0 = 20 \text{ mg}\cdot\text{L}^{-1}$ ;  $V = 250 \text{ mL}$ ).

To understand the adsorption mechanisms and the rate-limiting step, and to identify the kinetic parameters, numerous models were employed in the literature [5,63,64]. In the current study, four models were checked, namely, pseudo-first order, pseudo-second order, Elovich, and intraparticle diffusion. Table 4 summarizes the non-linear form of each equation with the regression coefficients and the corresponding parameters obtained from the fitting of the models to the experimental adsorption kinetic data.

Table 4. Adsorption kinetics modeling for the 2,4-D and carbofuran pesticides.

| Model                   | Non-Linear Expression   | Values of the Parameters                          |   | R <sup>2</sup> |         |
|-------------------------|---|---|---|----------------|---------|
|                         |   | 2,4-D   | Carbofuran  | 2,4-D          | Carbof. |
| Pseudo first-order      | $q_t = q_e \cdot (1 - e^{-k_1 t})$                                | T = 25 °C; $q_e = 271.4$ mg/g;<br>$k_1 = 0.073$   | T = 25 °C; $q_e = 134.2$ mg/g;<br>$k_1 = 0.048$   | 0.969          | 0.929   |
|                         |   | T = 45 °C; $q_e = 310.9$ mg/g;<br>$k_1 = 0.095$   | T = 45 °C; $q_e = 176.6$ mg/g;<br>$k_1 = 0.059$   | 0.979          | 0.988   |
|                         |   | T = 65 °C; $q_e = 340.7$ mg/g;<br>$k_1 = 0.112$   | T = 65 °C; $q_e = 234.9$ mg/g;<br>$k_1 = 0.058$   | 0.990          | 0.968   |
| Pseudo second-order     | $q_t = \frac{k_2 \cdot q_e^2 \cdot t}{1 + k_2 \cdot q_e \cdot t}$ | T = 25 °C; $q_e = 290.9$ mg/g;<br>$k_2 = 0.00035$ | T = 25 °C; $q_e = 149.5$ mg/g;<br>$k_2 = 0.00039$ | 0.961          | 0.915   |
|                         |   | T = 45 °C; $q_e = 330.0$ mg/g;<br>$k_2 = 0.00043$ | T = 45 °C; $q_e = 188.7$ mg/g;<br>$k_2 = 0.00045$ | 0.977          | 0.988   |
|                         |   | T = 65 °C; $q_e = 367.3$ mg/g;<br>$k_2 = 0.00047$ | T = 65 °C; $q_e = 242.2$ mg/g;<br>$k_2 = 0.00045$ | 0.980          | 0.916   |
| Elovich                 | $q_t = \frac{1}{\beta} \cdot \ln(1 + \alpha \cdot \beta \cdot t)$ | T = 25 °C; $\alpha = 202.7$ ;<br>$\beta = 0.026$  | T = 25 °C; $\alpha = 18.9$ ;<br>$\beta = 0.036$   | 0.900          | 0.860   |
|                         |   | T = 45 °C; $\alpha = 840.1$ ;<br>$\beta = 0.027$  | T = 45 °C; $\alpha = 62.2$ ;<br>$\beta = 0.034$   | 0.926          | 0.941   |
|                         |   | T = 65 °C; $\alpha = 822.1$ ;<br>$\beta = 0.022$  | T = 65 °C; $\alpha = 25.4$ ;<br>$\beta = 0.019$   | 0.936          | 0.866   |
| Intraparticle diffusion | $q_t = K_p \cdot \sqrt{t} + C$                                    | T = 25 °C;<br>$K_p = 10.19$ ; C = 110.1           | T = 25 °C;<br>$K_p = 7.02$ ; C = 32.1             | 0.618          | 0.685   |
|                         |   | T = 45 °C<br>$K_p = 10.73$ ; C = 145.5            | T = 45 °C<br>$K_p = 8.17$ ; C = 57.2              | 0.577          | 0.699   |
|                         |   | T = 65 °C<br>$K_p = 18.42$ ; C = 141.3            | T = 65 °C<br>$K_p = 12.61$ ; C = 49.6             | 0.588          | 0.683   |

According to the results, the pseudo first-order model yielded the best fitting for both 2,4-D and carbofuran adsorption on the activated carbon. Aksu et al. [64] found similar results for the adsorption of the 2,4-D on a commercial activated carbon. Meththika Vithanage et al. [65] confirmed that both pseudo first-order and pseudo second-order models described properly the kinetics of carbofuran adsorption. The intraparticle diffusion model does not fit properly with the experimental data (very low values of the correlation coefficients), suggesting that intraparticle diffusion is not the limiting step for the adsorption of both pollutants [66].

### 3.4. Thermodynamics

Temperature is a key parameter in adsorption since the change in temperature can modify the adsorption process, and consequently, the adsorption uptake. The thermodynamic parameters, standard free energy ( $\Delta G^0$ ), standard enthalpy ( $\Delta H^0$ ), and standard entropy ( $\Delta S^0$ ) were calculated for the following equations:

$$\Delta G^0 = -R \cdot T \cdot \ln(K_L) \quad (1)$$

$$\Delta G^0 = \Delta H^0 - T \cdot \Delta S^0 \quad (2)$$

where  $K_L$  is the Langmuir constant in ( $L \cdot mol^{-1}$ ) [67], T is the absolute temperature in kelvins, and R is the gas constant ( $8.314 J \cdot mol^{-1} \cdot K^{-1}$ ). Table 5 summarizes the values of the thermodynamic parameters obtained for the adsorption of both pesticides. The negative values of the standard free energy for both adsorbates are characteristic of spontaneous processes, as usual in adsorption.

**Table 5.** Thermodynamic parameters of the 2,4-D and carbofuran pesticide adsorption.

| Pollutant  | T (°C) | $\Delta G^0$ (kJ·mol <sup>-1</sup> ) | $\Delta H^0$ (kJ·mol <sup>-1</sup> ) | $\Delta S^0$ (kJ·mol <sup>-1</sup> ·K <sup>-1</sup> ) |
|------------|--------|--------------------------------------|--------------------------------------|---|
| 2,4-D      | 25     | −26.7                                | 16.9                                 | 0.146   |
|            | 45     | −29.2                                |                                      |   |
|            | 65     | −32.6                                |                                      |   |
| Carbofuran | 25     | −27.0                                | −22.4                                | 0.016   |
|            | 45     | −27.6                                |                                      |   |
|            | 65     | −27.7                                |                                      |   |

In the case of 2,4-D adsorption, the standard enthalpy is 16.9 kJ·mol<sup>-1</sup>. The positive value indicates that the adsorption process of this compound is endothermic, and the relatively low value is characteristic of predominantly physical adsorption. The standard entropy is −0.146 kJ·mol<sup>-1</sup>·K<sup>-1</sup>. The negative value is indicative of a decrease in the randomness of the molecules at the solid–liquid interface and a higher ordering of the 2,4-D molecules after being adsorbed on the activated carbon surface, although it should be considered that the value is very low, and consequently, indeed implies no significant change in entropy during adsorption. These results agree with other previous reports. In this sense, Kamaraj et al. [68] reported values of 0.13 kJ·mol<sup>-1</sup> and 0.412 kJ·mol<sup>-1</sup>·K<sup>-1</sup> for standard enthalpy and entropy, respectively, when analyzing the 2,4-D adsorption on metal hydroxides. A very similar value of the standard enthalpy 15.6 kJ·mol<sup>-1</sup> was obtained by Ding et al. [69] when analyzing the adsorption of 2,4-D on a magnetic ion-exchange resin, although they reported a low positive value of the standard entropy (0.076 kJ·mol<sup>-1</sup>·K<sup>-1</sup>). In the case of carbofuran, values of −22.4 kJ·mol<sup>-1</sup> and 0.016 kJ·mol<sup>-1</sup>·K<sup>-1</sup> were obtained for the standard enthalpy and entropy, respectively. The negative value of the standard enthalpy implies an exothermic adsorption process and again predominantly physical adsorption. The value of the standard entropy is very low, suggesting that the adsorption does not produce significant changes in the ordering of carbofuran molecules. The value of the standard enthalpy agrees with that reported by Mayakaduwa et al. [70] (−27.85 kJ·mol<sup>-1</sup>) for the carbofuran adsorption on an extruded activated carbon. Although, it should be noticed that this same study obtained positive standard enthalpy values for the adsorption of this same compound on a carbon black and a granular activated carbon (9.71 and 8.72 kJ·mol<sup>-1</sup>, respectively).

### 3.5. Adsorption Mechanism

At the adsorption pH used (c.a. 6.0), the activated carbon surface is negatively charged (see Figure 4) and 2,4-D and carbofuran molecules are in an anionic and molecular state, respectively. Considering this, in the case of 2,4-D, some repulsive interaction is expected between the carbon surface and the pesticide molecules, despite which high 2,4-D adsorption capacities have been observed. In the case of carbofuran, no significant electrostatic interaction is expected. This suggests that the adsorption mechanism of both pesticides is not governed by electrostatic forces. Most likely, a specific interaction between the oxygenated surface groups of the carbon surface and some groups of the molecules of the pesticides would take place, in addition to a physical adsorption process as suggested by the relatively low values of the standard adsorption enthalpies for both pollutants. Figure 6 represents the FTIR spectra of the activated carbon after adsorption of 2,4-D and carbofuran. In the case of 2,4-D adsorption, a new band is observed at 1474 cm<sup>-1</sup> that can be associated with the corresponding C=C vibration of the aromatic ring of the molecule, confirming the presence of the component of the carbon surface. However, no additional bands or significant modifications are observed which support the predominant physisorption of the 2,4-D molecules. The carbofuran adsorption results in the appearance of bands at 2964, 2920, and 2848 cm<sup>-1</sup> related to the stretching vibrations of C–H bonds in the pesticide molecule. In addition, a broadening and displacement of the stretching vibrations of the

O–H bonds up to  $3416\text{ cm}^{-1}$  can be observed, which suggest the participation of alcohols, phenols, and/or carboxylic acid groups in carbofuran adsorption via hydrogen bonding or dipole interactions [70].

#### 4. Conclusions

The chemical activation of peach stones with phosphoric acid resulted in carbons with well-developed surface area, obtaining the highest surface area ( $1182\text{ m}^2\cdot\text{g}^{-1}$ ) with an impregnation time of 5 h, an impregnation ratio equal to 3.5, an activation temperature of  $400\text{ }^\circ\text{C}$ , and 4.5 h of activation time. This carbon showed promising behavior for the adsorption of two model pesticides, 2,4-D and carbofuran. Adsorption kinetics confirmed that 2,4-D adsorption follows a pseudo first-order adsorption kinetic model, while carbofuran adsorption is better described by a pseudo second-order one. Regarding the equilibrium adsorption, a higher adsorption capacity is obtained for 2,4-D than carbofuran (c.a. 500 and  $250\text{ mg}\cdot\text{g}^{-1}$ , respectively). The analysis of the thermodynamics and characterization after use suggest a predominantly physisorption nature of the process. It should be considered that all the adsorption tests were performed with only one pollutant, future work should be performed in the evaluation of the performance of these carbon-based adsorbents in a more complex mixture of pollutants, and in the presence of other components usually found in natural waters. In addition, fixed-bed adsorption tests can be analyzed in the future to assess the interest of the proposed adsorbents in real practical applications.

**Author Contributions:** Conceptualization, C.B. and J.B.; methodology, S.H., A.Á.-M. and A.G.-A.; validation, S.H., A.Á.-M. and A.G.-A.; formal analysis, M.B., C.B. and J.B.; resources, C.B. and J.B.; writing—original draft preparation, S.H. and M.B.; writing—review and editing, A.Á.-M. and J.B.; supervision, S.G., C.B. and J.B.; project administration, S.G., C.B. and J.B.; funding acquisition, C.B. and J.B. All authors have read and agreed to the published version of the manuscript.

**Funding:** This research was funded by the Spanish “Agencia Estatal de Investigación” from “Ministerio de Ciencia e Innovación” proyect number TED2021-129948B-I00.

**Data Availability Statement:** Data are contained within the article.

**Conflicts of Interest:** The authors declare no conflicts of interest.

#### References

- Salomón, Y.L.D.O.; Georjina, J.; Franco, D.S.P.; Netto, M.S.; Picilli, D.G.A.; Foletto, E.L.; Oliveira, L.F.S.; Dotto, G.L. High-Performance Removal of 2,4-Dichlorophenoxyacetic Acid Herbicide in Water Using Activated Carbon Derived from Queen Palm Fruit Endocarp (*Syagrus romanzoffiana*). *J. Environ. Chem. Eng.* **2021**, *9*, 104911. [[CrossRef](#)]
- Rajeshkumar, S.; Mini, J.; Munuswamy, N. Effects of Heavy Metals on Antioxidants and Expression of HSP70 in Different Tissues of Milk Fish (*Chanos chanos*) of Kaattupalli Island, Chennai, India. *Ecotoxicol. Environ. Saf.* **2013**, *98*, 8–18. [[CrossRef](#)] [[PubMed](#)]
- Harabawy, A.S.A.; Ibrahim, A.T.A. Sublethal Toxicity of Carbofuran Pesticide on the African Catfish *Clarias Gariepinus* (Burchell, 1822): Hematological, Biochemical and Cytogenetic Response. *Ecotoxicol. Environ. Saf.* **2014**, *103*, 61–67. [[CrossRef](#)] [[PubMed](#)]
- Binh, Q.A.; Nguyen, H.H. Investigation the Isotherm and Kinetics of Adsorption Mechanism of Herbicide 2,4-Dichlorophenoxyacetic Acid (2,4-D) on Corn Cob Biochar. *Bioresour. Technol. Rep.* **2020**, *11*, 100520. [[CrossRef](#)]
- Salman, J.M.; Hameed, B.H. Adsorption of 2,4-Dichlorophenoxyacetic Acid and Carbofuran Pesticides onto Granular Activated Carbon. *Desalination* **2010**, *256*, 129–135. [[CrossRef](#)]
- Cotillas, S.; Sáez, C.; Cañizares, P.; Cretescu, I.; Rodrigo, M.A. Removal of 2,4-D Herbicide in Soils Using a Combined Process Based on Washing and Adsorption Electrochemically Assisted. *Sep. Purif. Technol.* **2018**, *194*, 19–25. [[CrossRef](#)]
- Ibrahim, K.E.A.; Şolpan, D. Removal of Carbofuran in Aqueous Solution by Using UV-Irradiation/Hydrogen Peroxide. *J. Environ. Chem. Eng.* **2019**, *7*, 102820. [[CrossRef](#)]
- Nejati, K.; Davary, S.; Saati, M. Study of 2,4-Dichlorophenoxyacetic Acid (2,4-D) Removal by Cu-Fe-Layered Double Hydroxide from Aqueous Solution. *Appl. Surf. Sci.* **2013**, *280*, 67–73. [[CrossRef](#)]
- Fiorenza, R.; Di Mauro, A.; Cantarella, M.; Privitera, V.; Impellizzeri, G. Selective Photodegradation of 2,4-D Pesticide from Water by Molecularly Imprinted  $\text{TiO}_2$ . *J. Photochem. Photobiol. A Chem.* **2019**, *380*, 111872. [[CrossRef](#)]
- Hameed, B.H.; Salman, J.M.; Ahmad, A.L. Adsorption Isotherm and Kinetic Modeling of 2,4-D Pesticide on Activated Carbon Derived from Date Stones. *J. Hazard. Mater.* **2009**, *163*, 121–126. [[CrossRef](#)]
- Goswami, B.; Mahanta, D. Polyaniline- $\text{Fe}_3\text{O}_4$  and Polypyrrole- $\text{Fe}_3\text{O}_4$  magnetic Nanocomposites for Removal of 2,4-Dichlorophenoxyacetic Acid from Aqueous Medium. *J. Environ. Chem. Eng.* **2020**, *8*, 103919. [[CrossRef](#)]

12. Mishra, S.; Zhang, W.; Lin, Z.; Pang, S.; Huang, Y.; Bhatt, P.; Chen, S. Carbofuran Toxicity and Its Microbial Degradation in Contaminated Environments. *Chemosphere* **2020**, *259*, 127419. [[CrossRef](#)] [[PubMed](#)]
13. Barbieri, E.; Ferrarini, A.M.T.; Rezende, K.F.O.; Martinez, D.S.T.; Alves, O.L. Effects of Multiwalled Carbon Nanotubes and Carbofuran on Metabolism in *Astyanax Ribeirae*, a Native Species. *Fish Physiol. Biochem.* **2019**, *45*, 417–426. [[CrossRef](#)] [[PubMed](#)]
14. Mansano, A.S.; Moreira, R.A.; Pierozzi, M.; Oliveira, T.M.A.; Vieira, E.M.; Rocha, O.; Regali-Selegim, M.H. Effects of Diuron and Carbofuran Pesticides in Their Pure and Commercial Forms on *Paramecium Caudatum*: The Use of Protozoan in Ecotoxicology. *Environ. Pollut.* **2016**, *213*, 160–172. [[CrossRef](#)]
15. Taher, T.; Munandar, A.; Mawaddah, N.; Syamsuddin Wisnubroto, M.; Siregar, P.M.S.B.N.; Palapa, N.R.; Lesbani, A.; Wibowo, Y.G. Synthesis and Characterization of Montmorillonite—Mixed Metal Oxide Composite and Its Adsorption Performance for Anionic and Cationic Dyes Removal. *Inorg. Chem. Commun.* **2023**, *147*, 110231. [[CrossRef](#)]
16. Mariana, M.; Abdul, A.K.; Mistar, E.M.; Yahya, E.B.; Alfatah, T.; Danish, M.; Amayreh, M. Recent Advances in Activated Carbon Modification Techniques for Enhanced Heavy Metal Adsorption. *J. Water Process Eng.* **2021**, *43*, 102221. [[CrossRef](#)]
17. Brishti, R.S.; Kundu, R.; Habib, M.A.; Ara, M.H. Adsorption of Iron(III) from Aqueous Solution onto Activated Carbon of a Natural Source: Bombax Ceiba Fruit Shell. *Results Chem.* **2023**, *5*, 100727. [[CrossRef](#)]
18. Subba Reddy, Y.; Matangi, R.; Rotte, N.K. Sustainable Mesoporous Graphitic Activated Carbon as Biosorbent for Efficient Adsorption of Acidic and Basic Dyes from Wastewater: Equilibrium, Kinetics and Thermodynamic Studies. *SSRN Electron. J.* **2022**, *9*, 100214. [[CrossRef](#)]
19. Sellaoui, L.; Yazidi, A.; Taamalli, S.; Bonilla-Petriciolet, A.; Louis, F.; El Bakali, A.; Badawi, M.; Lima, E.C.; Lima, D.R.; Chen, Z. Adsorption of 3-Aminophenol and Resorcinol on Avocado Seed Activated Carbon: Mathematical Modelling, Thermodynamic Study and Description of Adsorbent Performance. *J. Mol. Liq.* **2021**, *342*, 116952. [[CrossRef](#)]
20. Zhang, Z.; Wang, T.; Zhang, H.; Liu, Y.; Xing, B. Adsorption of Pb(II) and Cd(II) by Magnetic Activated Carbon and Its Mechanism. *Sci. Total Environ.* **2021**, *757*, 143910. [[CrossRef](#)]
21. Zhu, J.; Li, Y.; Xu, L.; Liu, Z. Removal of Toluene from Waste Gas by Adsorption-Desorption Process Using Corncob-Based Activated Carbons as Adsorbents. *Ecotoxicol. Environ. Saf.* **2018**, *165*, 115–125. [[CrossRef](#)] [[PubMed](#)]
22. Mansoorianfar, M.; Nabipour, H.; Pahlevani, F.; Zhao, Y.; Hussain, Z.; Hojjati-Najafabadi, A.; Hoang, Y.H.; Pei, R. Recent progress on adsorption of cadmium ions from water systems using metal-organic frameworks (MOFs) as an efficient class of porous materials. *Environ. Res.* **2022**, *214*, 114113. [[CrossRef](#)] [[PubMed](#)]
23. Hojjati-Najafabadi, A.; Mansoorianfar, M.; Liang, T.; Shahin, K.; Wen, Y.; Bahrami, A.; Karaman, C.; Zare, N.; Karimi-Maleh, H.; Vasseghian, Y. Magnetic-MXene-based nanocomposites for water and wastewater treatment: A review. *J. Water Process Eng.* **2022**, *47*, 102696. [[CrossRef](#)]
24. Nabipour, H.; Mansoorianfar, M.; Hu, Y. Carboxymethyl cellulose-coated HKUST-1 for baclofen drug delivery in vitro. *Chem. Pap.* **2022**, *76*, 6557–6566. [[CrossRef](#)]
25. Álvarez-Torrellas, S.; García-Lovera, R.; Escalona, N.; Sepúlveda, C.; Sotelo, J.L.; García, J. Chemical-activated carbons from peach stones for the adsorption of emerging contaminants in aqueous solutions. *Chem. Eng. J.* **2015**, *279*, 788–798. [[CrossRef](#)]
26. Mohammad, S.G.; El-Sayed, M.M.H. Removal of imidacloprid pesticide using nanoporous activated carbons produced via pyrolysis of peach stone agricultural wastes. *Chem. Eng. Commun.* **2021**, *208*, 1069–1080. [[CrossRef](#)]
27. Sanz-Santos, E.; Álvarez-Torrellas, S.; Larriba, M.; García, J. Activated carbons derived from biomass for the removal by adsorption of several pesticides from water. In *Advanced Materials for Sustainable Environmental Remediation*; Giannakoudakis, D., Meili, L., Anastopoulos, I., Eds.; Elsevier: Amsterdam, The Netherlands, 2022; pp. 565–583. ISBN 978032390485.
28. Bedia, J.; Bolver, C.; Ponce, S.; Rodriguez, J.; Rodriguez, J.J. Adsorption of Antipyrine by Activated Carbons from FeCl<sub>3</sub>-Activation of Tara Gum. *Chem. Eng. J.* **2018**, *333*, 58–65. [[CrossRef](#)]
29. Bedia, J.; Peñas-Garzón, M.; Gómez-Avilés, A.; Rodriguez, J.J.; Bolver, C. Review on Activated Carbons by Chemical Activation with FeCl<sub>3</sub>. *C—J. Carbon Res.* **2020**, *6*, 21. [[CrossRef](#)]
30. Hosseinzaei, B.; Hadianfard, M.J.; Ruiz-Rosas, R.; Rosas, J.M.; Rodríguez-Mirasol, J.; Cordero, T. Effect of Heating Rate and H<sub>3</sub>PO<sub>4</sub> as Catalyst on the Pyrolysis of Agricultural Residues. *J. Anal. Appl. Pyrolysis* **2022**, *168*, 105724. [[CrossRef](#)]
31. Rosas, J.M.; Ruiz-Rosas, R.; Rodríguez-Mirasol, J.; Cordero, T. Kinetic Study of SO<sub>2</sub> Removal over Lignin-Based Activated Carbon. *Chem. Eng. J.* **2017**, *307*, 707–721. [[CrossRef](#)]
32. Rosas, J.M.; Bedia, J.; Rodríguez-Mirasol, J.; Cordero, T. Hemp-Derived Activated Carbon Fibers by Chemical Activation with Phosphoric Acid. *Fuel* **2009**, *88*, 19–26. [[CrossRef](#)]
33. Kousha, M.; Tavakoli, S.; Daneshvar, E.; Vazirzadeh, A.; Bhatnagar, A. Central Composite Design Optimization of Acid Blue 25 Dye Biosorption Using Shrimp Shell Biomass. *J. Mol. Liq.* **2015**, *207*, 266–273. [[CrossRef](#)]
34. Bagheri, R.; Ghaedi, M.; Asfaram, A.; Alipanahpour Dil, E.; Javadian, H. RSM-CCD Design of Malachite Green Adsorption onto Activated Carbon with Multimodal Pore Size Distribution Prepared from *Amygdalus Scoparia*: Kinetic and Isotherm Studies. *Polyhedron* **2019**, *171*, 464–472. [[CrossRef](#)]
35. Pérez-Rodríguez, S.; Sebastián, D.; Alegre, C.; Tsoncheva, T.; Petrov, N.; Paneva, D.; Lázaro, M.J. Biomass Waste-Derived Nitrogen and Iron Co-Doped Nanoporous Carbons as Electrocatalysts for the Oxygen Reduction Reaction. *Electrochim. Acta* **2021**, *387*, 138490. [[CrossRef](#)]

36. Kozyatnyk, I.; Oesterle, P.; Wurzer, C.; Mašek, O.; Jansson, S. Removal of Contaminants of Emerging Concern from Multicomponent Systems Using Carbon Dioxide Activated Biochar from Lignocellulosic Feedstocks. *Bioresour. Technol.* **2021**, *340*, 125561. [[CrossRef](#)] [[PubMed](#)]
37. Sing, K.S.W. Reporting physisorption data for gas/solid systems with special reference to the determination of surface area and porosity (Recommendations 1984). *Pure Appl. Chem.* **1985**, *57*, 603–619. [[CrossRef](#)]
38. Calzaferri, G.; Gallagher, S.H.; Brühwiler, D. Multiple Equilibria Describe the Complete Adsorption Isotherms of Nonporous, Microporous, and Mesoporous Adsorbents. *Microporous Mesoporous Mater.* **2022**, *330*, 111563. [[CrossRef](#)]
39. Thommes, M.; Kaneko, K.; Neimark, A.V.; Olivier, J.P.; Rodriguez-Reinoso, F.; Rouquerol, J.; Sing, K.S.W. Physisorption of Gases, with Special Reference to the Evaluation of Surface Area and Pore Size Distribution (IUPAC Technical Report). *Pure Appl. Chem.* **2015**, *87*, 1051–1069. [[CrossRef](#)]
40. Pérez-Rodríguez, S.; Pinto, O.; Izquierdo, M.T.; Segura, C.; Poon, P.S.; Celzard, A.; Matos, J.; Fierro, V. Upgrading of Pine Tannin Biochars as Electrochemical Capacitor Electrodes. *J. Colloid Interface Sci.* **2021**, *601*, 863–876. [[CrossRef](#)]
41. Martins, A.F.; Villetti, M.A.; Mortari, S.R.; Pedroso, G.B.; Saldanha, L.F.; Rambo, M.K.D. Detoxification of Fermentable Broth with Activated Biocarbon Resulting from Pyrolysis of Agroforestry Residues. *Water Environ. Res.* **2021**, *93*, 1445–1454. [[CrossRef](#)]
42. Gerçel, Ö.; Özcan, A.; Özcan, A.S.; Gerçel, H.F. Capacity of Activated Carbon Derived from Peach Stones by  $K_2CO_3$  in the Removal of Acid, Reactive, and Direct Dyes from Aqueous Solution. *Environ. Eng.* **2009**, *135*, 919–932. [[CrossRef](#)]
43. Demiral, İ.; Samdan, C.; Demiral, H. Enrichment of the Surface Functional Groups of Activated Carbon by Modification Metho. *Surf. Interfaces* **2021**, *22*, 100873. [[CrossRef](#)]
44. Wang, H.; Xu, J.; Liu, X.; Sheng, L. Preparation of Straw Activated Carbon and Its Application in Wastewater Treatment: A Review. *J. Clean. Prod.* **2021**, *283*, 124671. [[CrossRef](#)]
45. Bedia, J.; Rosas, J.M.; Rodríguez-Mirasol, J.; Cordero, T. Pd Supported on Mesoporous Activated Carbons with High Oxidation Resistance as Catalysts for Toluene Oxidation. *Appl. Catal. B Environ.* **2010**, *94*, 8–18. [[CrossRef](#)]
46. Rosas, J.M.; Ruiz-Rosas, R.; Rodríguez-Mirasol, J.; Cordero, T. Kinetic Study of the Oxidation Resistance of Phosphorus-Containing Activated Carbons. *Carbon* **2012**, *50*, 1523–1537. [[CrossRef](#)]
47. Rosas, J.M.; Bedia, J.; Rodríguez-Mirasol, J.; Cordero, T. Preparation of Hemp-Derived Activated Carbon Monoliths. Adsorption of Water Vapor. *Ind. Eng. Chem. Res.* **2008**, *47*, 1288–1296. [[CrossRef](#)]
48. Njoku, V.O.; Islam, M.A.; Asif, M.; Hameed, B.H. Preparation of Mesoporous Activated Carbon from Coconut Frond for the Adsorption of Carbofuran Insecticide. *J. Anal. Appl. Pyrolysis* **2014**, *110*, 172–180. [[CrossRef](#)]
49. Calisto, J.S.; Pacheco, I.S.; Freitas, L.L.; Santana, L.K.; Fagundes, W.S.; Amaral, F.A.; Canobre, S.C. Adsorption Kinetic and Thermodynamic Studies of the 2, 4—Dichlorophenoxyacetate (2,4-D) by the [Co–Al–Cl] Layered Double Hydroxide. *Heliyon* **2019**, *5*, e02553. [[CrossRef](#)]
50. Samy, M.; Gar Alalm, M.; Fujii, M.; Ibrahim, M.G. Doping of Ni in MIL-125(Ti) for Enhanced Photocatalytic Degradation of Carbofuran: Reusability of Coated Plates and Effect of Different Water Matrices. *J. Water Process Eng.* **2021**, *44*, 102449. [[CrossRef](#)]
51. Zawadzki, J. Infrared Spectroscopy in Surface Chemistry of Carbons. *Chem. Phys. Carbon* **1989**, *21*, 147–386.
52. Puziy, A.M.; Poddubnaya, O.I.; Martínez-Alonso, A.; Suárez-García, F.; Tascón, J.M.D. Synthetic Carbons Activated with Phosphoric—Acid I. Surface Chemistry and Ion Binding Properties. *Carbon* **2002**, *40*, 1493–1505. [[CrossRef](#)]
53. Feng, P.; Li, J.; Wang, H.; Xu, Z. Biomass-Based Activated Carbon, and Activators: Preparation of Activated Carbon from Corncob by Chemical Activation with Biomass Pyrolysis Liquids. *ACS Omega* **2020**, *5*, 24064–24072. [[CrossRef](#)] [[PubMed](#)]
54. Bedia, J.; Peñas-Garzón, M.; Gómez-Avilés, A.; Rodriguez, J.; Belver, C. A Review on the Synthesis and Characterization of Biomass-Derived Carbons for Adsorption of Emerging Contaminants from Water. *J. Carbon Res.* **2018**, *4*, 63. [[CrossRef](#)]
55. Sun, Y.; Yue, Q.; Gao, B.; Huang, L.; Xu, X.; Li, Q. Comparative Study on Characterization and Adsorption Properties of Activated Carbons with  $H_3PO_4$  and  $H_4P_2O_7$  Activation Employing *Cyperus Alternifolius* as Precursor. *Chem. Eng. J.* **2012**, *181–182*, 790–797. [[CrossRef](#)]
56. Giles, C.H.; Silva, A.P.D.; Easton, I.A. A general treatment and classification of the solute adsorption isotherm part. II. Experimental interpretation. *J. Colloid Interface Sci.* **1974**, *47*, 766–778. [[CrossRef](#)]
57. Gómez-Avilés, A.; Peñas-Garzón, M.; Belver, C.; Rodriguez, J.J.; Bedia, J. Equilibrium, Kinetics and Breakthrough Curves of Acetaminophen Adsorption onto Activated Carbons from Microwave-Assisted  $FeCl_3$ -Activation of Lignin. *Sep. Purif. Technol.* **2022**, *278*, 119654. [[CrossRef](#)]
58. Gupta, V.K.; Ali, I.; Suhas; Saini, V.K. Adsorption of 2,4-D and Carbofuran Pesticides Using Fertilizer and Steel Industry Wastes. *J. Colloid Interface Sci.* **2006**, *299*, 556–563. [[CrossRef](#)] [[PubMed](#)]
59. Lazarotto, J.S.; da Boit Martinello, K.; Georgin, J.; Franco, D.S.P.; Netto, M.S.; Piccilli, D.G.A.; Silva, L.F.O.; Lima, E.C.; Dotto, G.L. Preparation of Activated Carbon from the Residues of the Mushroom (*Agaricus bisporus*) Production Chain for the Adsorption of the 2,4-Dichlorophenoxyacetic Herbicide. *J. Environ. Chem. Eng.* **2021**, *9*, 106843. [[CrossRef](#)]
60. Salman, J.M.; Njoku, V.O.; Hameed, B.H. Bentazon and Carbofuran Adsorption onto Date Seed Activated Carbon: Kinetics and Equilibrium. *Chem. Eng. J.* **2011**, *173*, 361–368. [[CrossRef](#)]
61. Al-Ghouti, M.A.; Da'ana, D.A. Guidelines for the Use and Interpretation of Adsorption Isotherm Models: A Review. *J. Hazard. Mater.* **2020**, *393*, 122383. [[CrossRef](#)]
62. Wang, J.; Guo, X. Adsorption Isotherm Models: Classification, Physical Meaning, Application and Solving Method. *Chemosphere* **2020**, *258*, 127279. [[CrossRef](#)] [[PubMed](#)]

63. Orduz, A.E.; Acebal, C.; Zanini, G. Activated Carbon from Peanut Shells: 2,4-D Desorption Kinetics Study for Application as a Green Material for Analytical Purposes. *J. Environ. Chem. Eng.* **2021**, *9*, 104601. [[CrossRef](#)]
64. Aksu, Z.; Kabasakal, E. Batch Adsorption of 2,4-Dichlorophenoxy-Acetic Acid (2,4-D) from Aqueous Solution by Granular Activated Carbon. *Sep. Purif. Technol.* **2004**, *35*, 223–240. [[CrossRef](#)]
65. Vithanage, M.; Mayakaduwa, S.S.; Herath, I.; Ok, Y.S.; Mohan, D. Kinetics, Thermodynamics and Mechanistic Studies of Carbofuran Removal Using Biochars from Tea Waste and Rice Husks. *Chemosphere* **2016**, *150*, 781–789. [[CrossRef](#)] [[PubMed](#)]
66. Rashidi, N.A.; Yusup, S.; Hameed, B.H. Kinetic Studies on Carbon Dioxide Capture Using Lignocellulosic Based Activated Carbon. *Energy* **2013**, *61*, 440–446. [[CrossRef](#)]
67. Liu, Y. Is the Free Energy Change of Adsorption Correctly Calculated? *J. Chem. Eng. Data* **2009**, *54*, 1981–1985. [[CrossRef](#)]
68. Kamaraj, R.; Davidson, D.J.; Sozhan, G.; Vasudevan, S. Adsorption of 2,4-Dichlorophenoxyacetic Acid (2,4-D) from Water by in Situ Generated Metal Hydroxides Using Sacrificial Anodes. *J. Taiwan Inst. Chem. Eng.* **2014**, *45*, 2943–2949. [[CrossRef](#)]
69. Ding, L.; Lu, X.; Deng, H.; Zhang, X. Aqueous Solutions Using MIEX Resin. *Ind. Eng. Chem. Res.* **2012**, *51*, 11226–11235. [[CrossRef](#)]
70. Mayakaduwa, S.S.; Herath, I.; Ok, Y.S.; Mohan, D.; Vithanage, M. Insights into Aqueous Carbofuran Removal by Modified and Non-Modified Rice Husk Biochars. *Environ. Sci. Pollut. Res.* **2017**, *24*, 22755–22763. [[CrossRef](#)]

**Disclaimer/Publisher’s Note:** The statements, opinions and data contained in all publications are solely those of the individual author(s) and contributor(s) and not of MDPI and/or the editor(s). MDPI and/or the editor(s) disclaim responsibility for any injury to people or property resulting from any ideas, methods, instructions or products referred to in the content.